ARMY RESEARCH LABORATORY

QWIP and MCT for Long Wavelength and Multicolor Focal Plane Array Applications

by Meimei Z. Tidrow

ARL-TR-1534 May 1998

The findings in this report are not to be construed as an official Department of the Army position unless so designated by other authorized documents.

Citation of manufacturer's or trade names does not constitute an official endorsement or approval of the use thereof.

Destroy this report when it is no longer needed. Do not return it to the originator.

Army Research Laboratory
Adelphi, MD 20783-1197

ARL-TR-1534 **May 1998**

QWIP and MCT for Long Wavelength and Multicolor Focal Plane Array Applications

Meimei Z. Tidrow
Sensors and Electron Devices Directorate

sponsored by

Ballistic Missile Defense Organization
7100 Defense Pentagon, Room 1E149
Washington, DC 20301-7100

Abstract

Infrared (IR) sensor technology is critical to all phases of ballistic missile defense. Traditionally, material systems such as indium antimonide (InSb), platinum silicide (PtSi), mercury cadmium telluride (MCT), and arsenic doped silicon (Si: As) have dominated IR detection. Improvement in surveillance sensors and interceptor seekers requires large, highly uniform, and multicolor (or multispectral) IR focal plane arrays involving mid-wave (MW), long-wave (LW), and very-long-wave (VLW) IR regions. Among the competing technologies are quantum-well infrared photodetectors (QWIPs) based on lattice-matched GaAs/AlGaAs and strained layer InGaAs/AlGaAs material systems. Even though QWIP cannot compete with MCT at the single device level (considering the quantum efficiency and D^*), it has potential advantages over MCT for LW and VLW focal plane array applications in terms of the array size, uniformity, operability, yield, reliability, and cost effectiveness. QWIPs are especially promising for VLWIR at low temperature operation, and when simultaneous multicolor detection with a single focal plane array is desired. Operating a VLWIR focal plane array at low background is a challenge to both MCT and QWIP, while QWIP has more potential to be realized due to its good properties at low temperatures. In this paper, I discuss cooled IR technology with an emphasis on QWIP and MCT. I give details concerning device physics, material growth, device fabrication, device performance, and cost effectiveness for LWIR, VLWIR, and multicolor applications.

Contents

Figures

1. Introduction

Infrared (IR) detection has been extensively investigated ever since the discovery of IR radiation in 1800. It has been used in both commercial and military applications. The IR spectrum can be divided into short-wave IR (SWIR) (1 to 3 μm), medium-wave IR (MWIR) (3 to 5 μm), long-wave IR (LWIR) (8 to 12 μm), and very-long-wave IR (VLWIR) (> 12 μm). Mercury cadmium telluride (MCT) is the most extensively investigated semiconductor alloy system for infrared detectors, with special consideration of its potential for LWIR and VLWIR applications. During more than 30 years of research, significant progress has been made in MCT materials, growth, processing, passivation, substrates, and manufacturing capability. In the SWIR range, large area format focal plane arrays (FPAs) have been demonstrated with formats of up to 1024×1024 pixels [1]. According to Compain and Boch from Sofradir and Leti [2], two-dimensional (2-D) arrays in MWIR can be found with up to 320×240 pixels for full performance and up to 640×480 pixels with limited performance. In LWIR, most of the arrays are limited to 320×240 pixels for full performance and 640×480 arrays for limited performance. The progress of MCT in the LWIR and VLWIR ranges has been relatively slow until the recent development of molecular beam expitaxy (MBE) growth technology. So far, 128×128 and 256×256 LWIR arrays with MBE for both planar [4] and mesa [5] structures have been demonstrated. A 128×128 pixel MCT array at 15 μm has also been demonstrated for a planar structure with MBE [6], which is a significant achievement for MCT technology. MBE technology gives MCT more potential to produce high-quality FPAs in LWIR, but the array size, uniformity, reproducibility, and yield are still difficult issues, considering the substrate problems, material properties, and array fabrication, especially for low temperature and low background operation. Extending to VLWIR and multicolor brings more challenges to MCT due to the even narrower band gap and more complicated device structures, especially at low temperatures for strategic applications.

The quantum-well infrared photodetector (QWIP) is a relatively new technology that has developed very quickly in the past 10 years [7]. N-type GaAs/AlGaAs and InGaAs/AlGaAs systems on GaAs substrates are the most studied and mature systems. Large area GaAs/AlGaAs FPAs with up to 640×480 pixels in LWIR [8, 9] and 128×128 pixels at 15 μm [10] have been demonstrated, with excellent uniformity and operability. Among the cooled IR detector systems, PtSi and InSb can be operated only in MWIR with no wavelength tunability and multicolor capabilities. Si:As has a wide band spectrum from 0.8 to 30 μm, but no tunability or multicolor capability has been developed. It can be operated only at temperatures around 12 K. Both MCT and QWIP offer wavelength flexibility in MWIR, LWIR, and VLWIR, as well as multicolor capabilities. In this paper, the discussion will be concentrated on these two IR systems at LWIR, VLWIR, and multicolor with emphasis on low temperature and low background applications. The fundamental problems of each system and how they affect the device performance and applications will be discussed.

2. Material Properties

Both QWIP and MCT are semiconductor IR devices. High-quality semiconductor materials are essential to the device performance and array production. The main requirements of IR materials are low defects; large wafers; and the reliability, uniformity, and reproducibility of intrinsic and extrinsic properties.

MCT has been considered the most important, yet most challenging, material for IR detection. The fundamental advantage of MCT is its direct interband transition with adjustable band gap. By properly controlling the composition x and operation temperature in $Hg_{1-x}Cd_xTe$, one can vary the band gap of MCT from 0 eV (x = 0) to 1.45 eV (x = 1 at 77 K), which theoretically could cover IR ranges from 1 to 50 μm. Other advantages of MCT include small effective mass, high electron mobility, and long minority carrier lifetime. All these advantages contribute to a very high quantum efficiency of around 70 percent and a relatively small thermally generated dark current at a temperature (T) higher than 77 K.

However, MCT has very serious technological problems in mass production [11]. The natural band gap of MCT is very narrow at LWIR (0.124 eV at 10 μm cutoff, 0.082 eV at 15 μm cutoff), which makes the material system unstable. HgTe is a semimetal in which the bond of Hg-Te is very weak and is destabilized further by alloying it with CdTe. The high mercury vapor pressure and the HgCdTe phase diagram shape result in serious difficulties in repeatable and uniform growth [12, 13]. The soft but brittle nature of the MCT material and substrates makes the device processing difficult. Significant progress has been achieved in material and device qualities; however, difficulties still exist due to lattice, surface, and interface instabilities. Problems also remain in material properties, such as the roles of various impurities, dopant behavior, crystal growth, native defect chemistry, surface science, junction formation, passivation, and contact technology. Improved understanding of MCT material properties and how they affect the device performance is still critical to the continued development of MCT technology, especially for LWIR, VLWIR, and multicolor applications.

QWIPs use intersubband transition instead of direct interband transition. III-V materials are used, and these have a relatively wide band gap (1.43 eV for GaAs). The advantages of a wider band gap material are that it has superior bond strength and material stability, well-behaved dopants, thermal stability, and intrinsic radiation hardness. Large and high-quality GaAs substrates and mature GaAs growth and processing technology guarantee highly uniform, large area FPAs with well-controlled molar compositions. No passivation is needed in QWIP. The hardness of the material and substrate makes device processing and array fabrication easy to handle, which leads to a high yield for the FPAs. The disadvantage of this wider band gap material is that the energy band gap does not fall in the IR regime, and direct band gap transition cannot be used, for IR detection. Intersubband transition is used, which sets certain fundamental limits on the device performance at T > 80 K. Figure 1 shows the energy band gaps of MCT and QWIP materials.

Figure 1. The band gaps of MCT and QWIP materials.

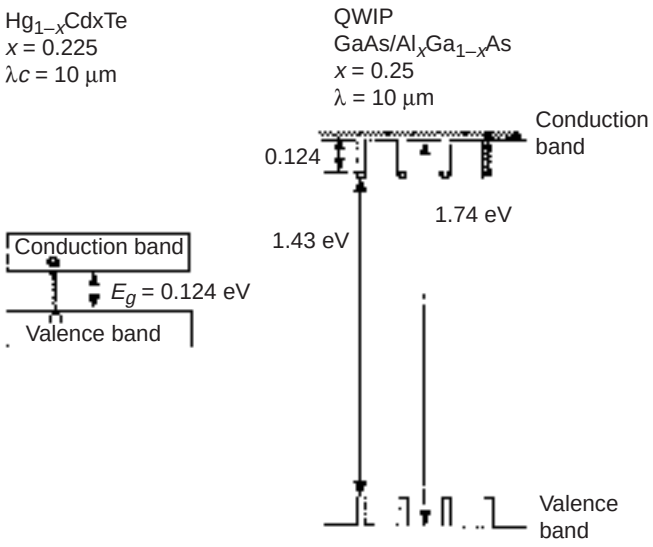

3. Basic Device Physics

MCT IR detectors could be operated either as a photoconductor or a photodiode. In the second-generation staring FPA applications, MCT photodiodes with a photovoltaic (PV) effect are preferred over photoconductors. The advantages are their relatively high R_oA (the dynamic resistance at zero bias voltage) product and lower power consumption compared with MCT photoconductors. The major problem with a photodiode is its involvement with p-type materials. Basic MCT photodiodes consist of either p-on-n or n-on-p, homo- or heterojunctions. For wavelengths from 2 to 20 μm at 77 K, n-type bases are favorable due to the lower and controllable doping. Heterojunctions usually exhibit higher R_oA products than homojunctions [14]. The devices could be either in planar or mesa formats. The operation of a basic p-n junction photodiode with the band gap diagram is illustrated in figure 2. An internal potential barrier is built due to the carrier diffusion. IR photons with energy larger than the band gap are absorbed by the photodiode and excite electrons in the valence band to the conduction band. If the absorption occurs within the depletion region, the electron-hole pairs are immediately separated by the strong built-in electric field and contribute to photocurrent in the external circuit. If the absorption occurs within one diffusion length of the depletion edge, the excited electron-hole pairs will diffuse to the depletion region first, where they are then separated by the electric field and contribute to photocurrent.

A QWIP takes advantage of band gap engineering so that wider band gap materials can be used. The fundamental difference between a QWIP and MCT is that a QWIP uses intersubband transitions with energy bands either in the conduction band (n-type) or in the valence band (p-type). A typical QWIP consists of 30 to 50 quantum-well periods. In an n-type GaAs/AlGaAs system, the intersubband transition happens only in the conduction band that involves electrons. By changing the Al concentration x, the band gap of $Al_xGa_{1-x}As$ can vary from 1.43 eV (x = 0) to 2.16 eV (x = 1) at 300 K. Using GaAs as the well region and AlGaAs as the barrier region, confined quantum-well structures can be formed when the well width is small. The thickness of the GaAs layer determines the well width

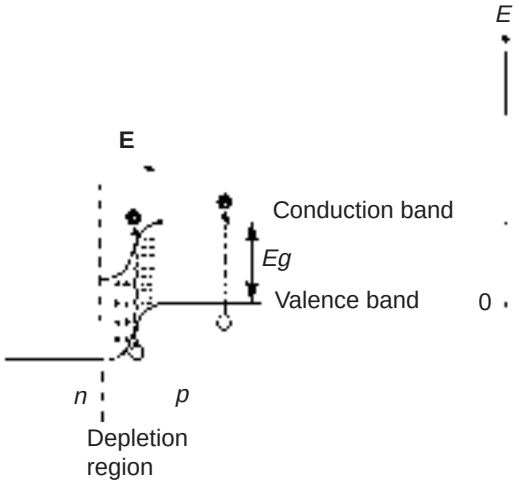

Figure 2. The band gap diagram of a basic p-n junction photodiode.

d, and the Al *x* value determines the barrier height *H*. QWIP devices are all in a mesa format. Figure 3 gives the device structure and band gap diagram for an n-type GaAs/AlGaAs QWIP under bias. The well region has one bound state as ground state and one or more excited states, depending on the barrier structure. The quantum wells are doped with electrons with Fermi energy above the ground state. IR photons with energy coinciding with the energy difference between the excited and ground states can be absorbed by electrons. QWIPs usually operate in the photoconductive mode, and bias voltage is applied to sweep the excited electron out of the well region. Depending on the position of the excited states in the well region, the intersubband transitions can be defined as bound-to-bound, bound-to-quasi-bound, and bound-to-continuum states. Figure 4 shows the three most commonly used QWIP structures: bound-to-quasi-bound [15], bound-to-continuum [16], and bound-to-miniband [17] transitions. By designing different well widths and barrier heights, one can achieve QWIP detection from 3 to 20 μm or even longer. With different combinations of barriers and well structures, different detection wavelengths, detection bandwidths, and multicolor combinations can be achieved.

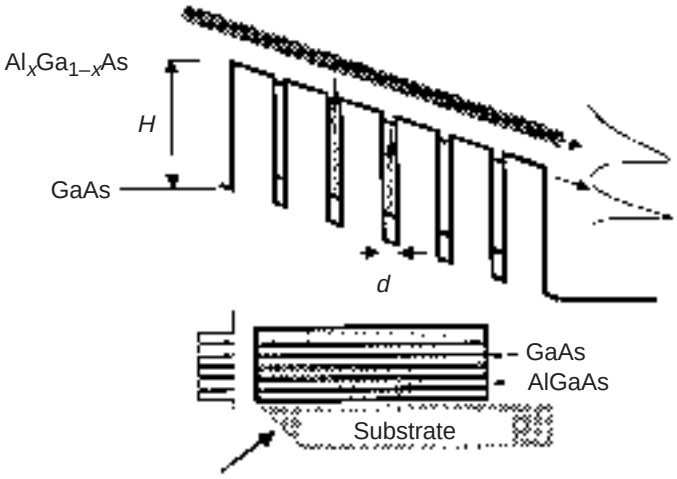

Figure 3. The device structure and band gap diagram of an n-type GaAs/AlGaAs QWIP under bias condition.

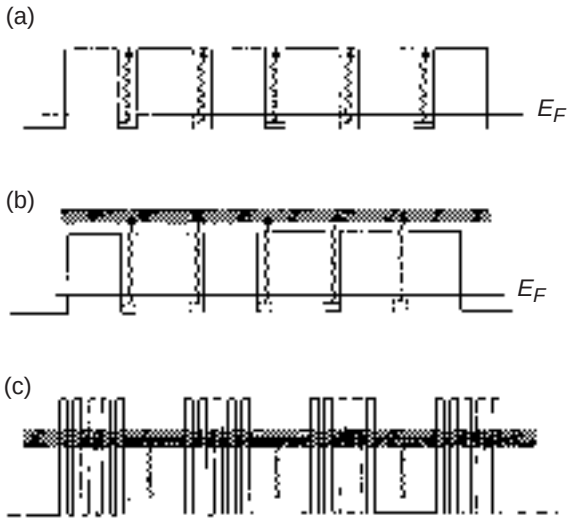

Figure 4. Three most commonly used QWIP structures: (a) bound-to-quasi-bound, (b) bound-to-continuum, and (c) bound-to-miniband transitions.

4. Device Fabrication

4.1 Substrates

Epitaxial techniques are necessary for crystal growth for FPA applications when large area epilayers and sophisticated layered structures are required with abrupt interfaces, complex compositions, good doping uniformity, and well-controlled layer thickness. One problem with epitaxial techniques is the need for an affordable, large area substrate that is structurally, chemically, optically, and mechanically matched to the device material. The quality of the substrates is very important because defects and crystalline imperfections in the substrates could propagate into the epitaxy layers.

For MCT, no substrate satisfies all the requirements [18]. CdZnTe is the most frequently used substrate for MCT. It has the metallurgical compatibility and lattice match with MCT that permit the growth of relatively higher quality epitaxial layers of MCT. But the available substrates are relatively small, soft, fragile, and expensive (about $700 for 1 in.^{2} polished). The typical dislocation concentration of CdZnTe [19] is $10^4/cm^2$ to $10^5/cm^2$, which allows the growth of good quality MCT at MWIR and LWIR for tactical applications. But it may not be pure enough for low background, low temperature, and VLWIR applications.

For the GaAs/AlGaAs material system used in QWIPs, GaAs substrates have a perfect lattice match with all Al concentrations. Large (6 in. diam) and high-quality GaAs substrates are available at a much lower cost than CdZnTe (about $150 for a 3 in. diam. wafer). For the InGaAs/GaAs system on GaAs, there is a limit on the indium concentration and layer thickness because of the lattice mismatch. Highly strained layers with 35 percent indium concentration have been grown, and the devices show very high-quality material [20, 21].

Both thermal expansion coefficients of GaAs and CdZnTe are poorly matched with Si readout. Substrate thinning or total removal has been a standard practice in FPA fabrication that somewhat relieves the strain and stress caused by the thermal expansion. GaAs can sustain more strain and stress due to its strong chemical bonds and durable mechanical properties, besides the thinner layers of QWIP compared to MCT. Alternative substrates for MCT have the potential to reduce the substrate cost, make large area arrays, and match to the readout. The most studied alternative substrates for MCT are Si, GaAs, and sapphire. Si is the more desirable substrate and is being heavily pursued. A sapphire substrate has shown the most success with a 1024×1024 pixel FPA demonstrated at 3.2 μm cutoff [1]. The limitation of the sapphire substrate is its cutoff wavelength in MWIR. Overall, the quality of the devices grown on alternative substrates is inferior to those grown on CdZnTe [3]. Major problems are the large lattice mismatch and thermal mismatch between the substrate and MCT material, which produce dislocations and affect the quality of the devices.

4.2 Material Growth

For an MCT photodiode, the active and capping layers can be grown with either LPE, metal-organic chemical vapor deposition (MOCVD), or MBE. The unstable nature of Hg in the system makes the control of composition, doping, and interface profiles very difficult when the material is grown, especially for reproducible LWIR, VLWIR, and multicolor devices. LPE, the most mature technology for MCT growth, has been used routinely for large volume production in SWIR, MWIR, and LWIR linear arrays. A 640×480 pixel LWIR FPA has used LPE growth [3]. The major problem with LPE is the precise control of x across the $Hg_{1-x}Cd_xTe$ wafer, which causes spectral nonuniformity, especially at LWIR and VLWIR. Precise control of the layer thickness and interface is another problem that makes the extension of MCT to multilayered multicolor devices difficult. The advantages of MBE are that it offers low temperature growth within an ultra-high vacuum environment; in situ n-type and p-type doping; and precise control of composition, doping, and interfacial profiles. However, because Hg has both a high vapor pressure and low sticking coefficient, the growth temperature must be very low (<200 °C). Special Hg sources are required in the MBE system, which make the system more complicated and costly than regular MBE for III-V material growth. So far, the device performance of MBE growth and LPE growth is comparable [5] in the LWIR. In the VLWIR, MBE has demonstrated 128×128 pixel arrays at 15 μm, which is one step ahead of LPE. MBE technology has the potential to improve the MCT material quality and device performance for VLWIR and multicolor devices.

The junctions of an epilayer MCT diode can be formed by ion implantation or in situ doping during the active and cap layer growth. The ion implantation has an advantage in that it is a planar process and requires only a simple surface passivation. Its disadvantages are that it is difficult to totally repair any damage created during the process and it is nearly impossible to use the process to build multilayer structures for advanced detectors. The advantage of the in situ doping approach is that it is a simple layer-by-layer growth process, so it is relatively easier to build a multilayer structure. The challenge of the in situ doping approach is that it requires tight control of growth temperature and fluxes and has a rather narrow window for the optimal growth. In addition, it requires a very stringent passivation for mesa structures [5].

For QWIPs of GaAs/AlGaAs, MBE is used to precisely lay the atomic layers down to form the quantum wells. The GaAs MBE growth technology is a very mature and proven technology in III-V electronic industry and monolithic microwave integrated circuit (MMIC) applications. The MBE technology ensures the success and repetition of the material growth and has precise control of layer thickness, chemical concentration, and doping profile. In order to produce the detection wavelength for MWIR, InGaAs/AlGaAs is usually used to increase the well depth. Strain is introduced during growth due to the lattice mismatch between GaAs and InGaAs. There is a critical thickness that can be grown pseudomorphically, depending on the indium concentration. Two-stack, two-color

QWIPs with 35 percent indium concentrations have been grown with 3 quantum wells in each stack and 20 quantum wells in each stack. The devices demonstrated excellent performance, which provided very high-quality material growth [20, 21].

4.3 Processing

Due to the unstable nature of the material and the mechanically soft yet brittle wafer and substrate, MCT is hard to handle and difficult to process in general. Because of the weak bond of HgCdTe, the chemical etching is very sensitive to the etching solution and the process, which affect the uniformity, yield, and reproducibility. Dry etching has proven to be more successful than wet etching. The band bending at the surface gives MCT a surface-leakage problem; hence, the surface passivation is needed for MCT arrays. Passivation is a critical step in MCT photodiode technology that greatly affects surface-leakage current and the device's thermal stability. Passivation of photodiodes is very difficult, because the same coating must simultaneously stabilize regions of n- and p-type materials. Some widely used passivation material for n-type MCT, such as anodic oxide, causes an inversion layer on a p-type material and cannot be used for junction devices [22]. Tremendous progress has been made in passivating MCT diodes with CdZnTe.

Device processing and array fabrication for QWIPs use standard III-V processing technology, which is very mature and highly repeatable. Any laboratory with a decent clean room should be able to process QWIP devices. No surface passivation is needed. For n-type GaAs/AlGaAs and InGaAs/AlGaAs systems, normal incidence is forbidden due to the selection rules, and extra grating processing is needed to effectively couple IR light into the detectors. Grating layers introduce extra steps into the processing but add no fundamental difficulties to the standard procedures.

5. Device Performance

5.1 Quantum Efficiency and Responsivity

MCT is an intrinsic detector that uses band-to-band transition. It has a large IR absorption and a wide absorption band. The quantum efficiency of MCT is very high, around 70 percent. When operated in the PV mode, the optical gain is one. The responsivity is directly proportional to the quantum efficiency of the device. High quantum efficiency is always desirable for single devices and scanning arrays. However, the current staring array performance is mostly limited by the charge handling capacity on the readout circuit and the warm optics at the background. Adjustable quantum efficiency sometimes is desirable to suit the integration time, while maintaining a certain signal-to-noise ratio.

N-type QWIPs use intersubband transitions in the conduction band. IR photons in resonance with the energy spacing between the ground state and excited state can be absorbed. The absorption quantum efficiency is relatively small, about 25 percent with 2-D grating. Although the spectral bandwidth is adjustable, overall it is much narrower than that of MCT. The quantum mechanical rules forbid normal incidence absorption. Even though normal incidence absorption without grating has been observed [20, 23], the value is relatively small and the physics behind it is not yet understood. Different gratings have been used with 1-D, 2-D, ring, checkboard [23, 24, 25], and random gratings [26]. New grating designs that improve the quantum efficiency are being studied, such as Enhanced QWIP [27], antenna grating [28], and corrugated grating [29]. Because QWIP is a photoconductor, the responsivity is proportional to the conversion efficiency, which is the product of the absorption quantum efficiency times the optical gain. The optical gain is defined as the ratio of the photoelectron lifetime to the transit time. The optical gain in a bound-to-miniband QWIP is around 0.2 with 50 wells. Other QWIP structures have demonstrated optical gain values from 0.2 to greater than 1.

The typical conversion efficiency of a regular QWIP array is less than 6 percent. However, one fact that has been neglected is that most efforts on QWIP are for tactical applications. The structure designs and the doping are optimized to increase the operating temperature and suit the readout charge handling capacity. A smaller number of quantum wells and bound-to-continuum structures could increase the optical gain and improve the detector performance for low temperature applications. With slightly increased doping density, a three-well QWIP (S-QWIP) has been demonstrated with high performance and a 29-percent conversion efficiency [30]. By optimization of the device structure, the number of wells, the doping density, and the new grating schemes, improvement in QWIPs' conversion efficiency is expected. The conversion efficiency, along with the dark current of a QWIP, can be tailored to suit the desired integration time for specific applications. Due to its intersubband nature, however, it is very hard for a QWIP to achieve a quantum efficiency at MCT's level.

5.2 Dark Current and R_oA

Dark current and R_oA products are important figures of merit in the evaluation of device performance. They reflect the quality of the material and device design. R_oA is defined as the dynamic resistance at zero bias voltage for PV devices. A QWIP is a photoconductor; the impedance $R_D = V/I_D$ is commonly used to evaluate the device's quality and ability to match the readout. $R_DA = V/J_D$ could be used for comparison with MCT with specified bias V and dark current density J_D. The major effects of the dark current are that, first, it causes noise and therefore reduces the signal-to-noise ratio; second, it fills the charge well of the readout capacitor.

The dark current in a photodiode can consist of diffusion current, generation-recombination (*g-r*) current, tunneling current, and surface-leakage current. Diffusion current is the fundamental current mechanism in a p-n junction photodiode. It arises from the random thermal generation and recombination of electron-hole pairs within a minority-carrier diffusion length on either side of the depletion region. The *g-r* current appears at the depletion region in which the Auger process is the only fundamental limit to device performance. Other mechanisms of *g-r* current, such as Shockley-Reed-Hall (SRH), are not intrinsic and should be able to be reduced with progress toward purer and higher quality materials. The tunneling current is caused by direct tunneling of electrons across the junction from the valence band to the conduction band (direct tunneling) or indirect tunneling through trap-assisted tunneling. Actual p-n junctions often have additional dark current, particularly at low temperature, which is related to the surface. Surface phenomena play an important role in the determination of PV detector performance. The surface of actual devices is passivated in order to stabilize the surface against chemical and heat-induced changes as well as to control surface recombination, leakage, and related noise.

In MCT diodes, the dark current sources could come from diffusion; *g-r*; band-to-band tunneling; trap-assisted tunneling; and leakages due to dislocations, precipitates, and surface and interface instabilities. The dark current could come from the base and cap layers, depletion layers, surfaces, and contact regions. From Rogalski (fig. 11.44 and table 11.4 [11]), one could get an idea of the main sources of a photodiode dark current. In MCT, the Auger mechanism governs the high temperature lifetime, and the SRH mechanism is mainly responsible for low temperature lifetimes. The *g-r* current varies with T as n_i, and is less rapid than diffusion current, which varies as n_i^2, where n_i is the intrinsic carrier density. Thus, a temperature is finally reached at which the two currents are comparable, and below this temperature the *g-r* current dominates [3]. At low temperature, such as 40 K, large spreads in R_oA distributions are typically observed due to the onset of tunneling currents associated with localized defects [31]. The tunneling mechanism is still not well understood, and it varies from diode to diode.

Single MCT devices are operated at near zero bias and R_oA is commonly used as the figure of the merit for the device quality. Top quality MCT diodes have shown R_oA products close to the theoretical limit. For example, a 10-μm cutoff MCT diode at 77 K has shown R_oA = 665 Ωcm^2 at 0 bias [32], which is within a factor of two of that predicted for the Auger 7 limit. In practice, the nonfundamental sources dominate the dark current of the present MCT photodiodes, with the exception of specific cases of near room temperature devices and highest quality 80 K LWIR and 200 K MWIR devices [11]. Typical values of R_oA at 77 K as a function of cutoff are given by Wu (fig. 1 [5]), including both LPE and MBE growth. From the figure, one can see that the average R_oA at 10 μm is around 300 Ωcm^2 and drops to 30 Ωcm^2 at 12 μm. At 40 K, the R_oA varies between 10^5 and 10^8 Ωcm^2 with 90 percent above the 10^5 Ωcm^2 at 11.3 μm [31]. For MCT FPA operation, certain bias is necessary to ensure a uniform responsivity of each device in the FPA. The R_oA product is supposedly increased with a small negative bias, but the actual FPA has shown larger leakage current and smaller R_oA. A good quality 128 × 128 pixel FPA grown by MBE from Hughes Research Center gives an R_oA of 220 Ωcm^2 at 80 K with 9.92-μm cutoff [33]. Santa Barbara Research Center's LPE growth shows similar values [3]. The LWIR 128 × 128 pixel FPA grown by MBE at Rockwell International has an R_oA of 83 Ωcm^2 at 80 K with 10.1-μm cutoff [4]. The LWIR R_oA in a two-color MCT is usually lower than the single color LWIR R_oA, indicating a lower quality of two-color devices. For example, the R_oA product is 100 Ωcm^2 for the LWIR of a two-color device from Hughes Research Center grown by MBE. In an MOCVD-grown two-color MCT structure from Lockheed Martin, the R_oA product of the LWIR is 16 Ωcm^2 at 80 K with 10.5-μm cutoff [34]. The dark current of the LWIR of this two-color device at 77 K is around 10 nA with a 75 × 75 μm^2 pixel array, which gives a dark current density of 2×10^{-4} Acm^{-2}. This value is similar to that of a QWIP at 77 K.

The behavior of the dark current of a QWIP is better understood. It has three mechanisms, as shown in figure 5. Usually one mechanism dominates at one temperature range even though all three mechanisms contribute at all temperatures. At low temperatures (T < 40 K for 10-μm cutoff), the dark current is mostly caused by defect-related direct tunneling (DT). With high-quality III-V material growth and processing, this dark current is very small. A typical LWIR QWIP at 40 K has a tunneling current density of 10^{-7} Acm^{-2}, which is smaller than 1 pA for a 24 × 24 μm^2 pixel. In the medium operating temperature range (40 to 70 K for 10-μm

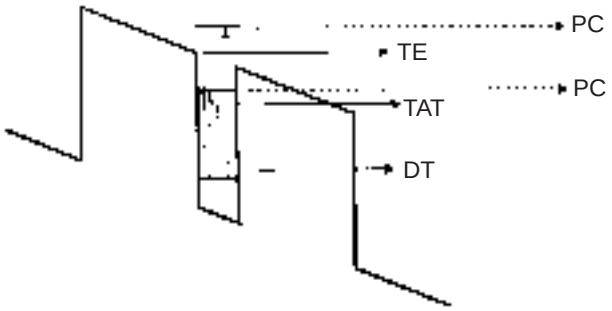

Figure 5. Three dark current mechanisms of QWIP, where DT is direct tunneling, TAT is thermally assisted tunneling, TE is thermionic emission, and PC is photocurrent.

cutoff), the thermally assisted tunneling (TAT) dominates. Electrons are thermally excited and tunnel through the barriers with assistance from the defects and the triangle part of the barrier at high bias. At high temperature (>70 K for 10-μm cutoff), thermally excited electrons are thermionically emitted (TE) and transport above the barriers. The value of the dark current could be adjusted with different device structures, doping densities, and bias conditions. For TE current, the dark electrons have energy and, therefore, transport mechanisms similar to photoelectrons. It is very hard to block this dark current without sacrificing the photoelectrons. Typical LWIR QWIP dark current density at 77 K is about 10^{-4} Acm^{-2}, which is in the nA range for a 24×24 μm^2 pixel. QWIP is a photoconductor that operates at a bias voltage from 1 to 3 V depending on the structure and the periods of the devices. With the voltage divided by the dark current density, the R_0A products are usually larger than 10 $M\Omega cm^2$ and 10 $k\Omega cm^2$ when operated at 40 and 77 K, respectively; this reflects very high impedance.

Due to the nature of intersubband transitions, the lifetime of thermal electrons is very short (<100 ps) in a QWIP; thus, they produce a larger thermal generation current than MCT. An estimate by Kinch and Yariv in 1989 [35] gave a dark current of a QWIP that was five orders of magnitude higher than that of MCT at 77 K. Improved material growth, device design, and optimized doping made this value much smaller, only 10 times larger [36] at 77 K. Therefore, a high-quality MCT diode should have a dark current 10 times smaller than a QWIP's at 77 K. At a relatively high temperature (>80 K), MCT's dark current is diffusion-limited and fairly uniform. For extremely high-quality MCT devices, this temperature could go down to 65 K. The intrinsically long lifetime of hot electrons in MCT determines that this dark current is much smaller than a QWIP's. The dark current of a QWIP might be able to be further suppressed to meet the system requirement at $T > 80$ K, but it is very hard to compete with MCT in this temperature range. At low temperature operation, the thermally generated dark current in QWIPs is reduced exponentially and maintains very good uniformity down to 40 K.

5.3 Noise

Detector noise can be distinguished in two types: radiation noise and intrinsic detector noise. Radiation noise includes signal fluctuation noise and background fluctuation noise. Intrinsic detector noise could have many sources, such as shot noise, Johnson noise, *g-r* noise, $1/f$ noise, and pattern noise. Johnson noise is the minimum intrinsic noise at zero bias. Usually, shot noise is the major noise for photodiodes, and *g-r* noise and Johnson noise are the major noises for photoconductors. However, MCT also has large Johnson noise and *g-r* noise due to the low R_0A product and the material problems. For FPAs, the pattern noise is the major limitation to an array's performance at low temperature. The fixed pattern noise results from local variation of the dark current, photoresponse, and cutoff wavelengths.

In QWIPs, the dark current is the major source that causes noise. Johnson noise is neglected in most cases, especially at high temperature operation due to the high dark current. But when the operation temperature goes down and the array pixel size gets smaller, Johnson noise becomes comparable to dark current noise and must be considered in noise calculations. Fixed pattern noise is also a limiting factor for QWIP array performance, but it is much smaller than that of MCT due to its material quality and better controlled cutoff wavelength. There is very little $1/f$ noise observed in QWIPs due to their stable surface properties.

5.4 BLIP Temperature

The background limited photodetection (BLIP) temperature is the temperature at which the dark current of the detector equals the background photocurrent, given a field of view (FOV), and a background temperature. BLIP is usually desirable but becomes more difficult with low background radiation. For a high-quality MCT diode, the dark current is 10 times smaller than that for a QWIP at 77 K, and its quantum efficiency is about 10 times larger. Even for a poor quality MCT with dark current similar to a QWIP's at 77 K, the BLIP temperature of MCT is usually still higher than that of a QWIP with a 300 K background. When the background goes lower, the dark current has to be reduced in order to achieve BLIP conditions. From 77 K to 40 K, a QWIP's dark current reduces three orders of magnitude uniformly, while MCT's dark current is SRH and tunneling limited and will vary from diode to diode. Thus, QWIP has the potential to perform better than MCT at low background and low temperature operation.

5.5 *D**

The D^* is an important figure of merit in evaluating IR detectors at single device level. It reflects the signal-to-noise ratio at a certain temperature with unit noise bandwidth and detector area. Under BLIP conditions, the D^*_{Blip} is determined by the quantum efficiency (or conversion efficiency for QWIP) and the background flux. With a 300 K background under BLIP operations, the D^* of a single MCT device is usually higher than that of a QWIP due to its higher quantum efficiency. When the temperature goes down, the tunneling current in MCT dominates, and the D^* of QWIP could be higher than MCT [37] and is definitely more uniform. At 77 K, the D^* of a LWIR QWIP is about 10^{10} cmHz$^{1/2}$W^{-1}, which could lead to a very good thermal imaging with noise equivalent temperature difference (NEDT) of 15 mK[7] for thermal imaging. When D^* is beyond a certain limit, increasing D^* will no longer increase array performance. In this situation, the array performance is uniformity limited [7].

6. Focal Plane Array

Besides the detector performance, major concerns in FPA applications are the array size, uniformity, operability, integration time, and matching to the readout circuit.

6.1 Uniformity

The uniformity among pixels within an array is important for accurate temperature measurements, background subtraction, and threshold testing. High uniformity and operability are extremely important for tracking and discriminating multiple unresolved targets. Dead pixels in an array could totally miss a target during the tracking, and the nonuniformity of an array increases the false alarm rate. FPA evaluations show that the fixed pattern noise is one of the main factors limiting the array performance [38]. The fixed pattern noise is a nonuniformity appearing across the array that does not vary with time. It reflects the intrinsic properties of an FPA. The nonuniformity value is usually calculated with the standard deviation over mean, counting the number of operable pixels in an array. For the same array, the nonuniformity can be different depending on the specification of operability. For example, a higher requirement on the operability usually leads to a lower uniformity and vice versa. Beck et al. (fig. 7 [39]) shows the corrected response nonuniformity as a function of the number of bad pixels. In the figure, the corrected responsivity nonuniformity of the center 64×64 pixels in a 256×256 pixel QWIP array by Lockheed Martin is 0.04 percent with 10 pixels excluded; this means 99.75 percent operability. If only 4 pixels are excluded—99.90 percent operability—the nonuniformity is increased to 0.045 percent. The nonuniformity (and operability) directly affects the NEDT or noise equivalence irradiance (NEI) and, thus, the array performance.

Because of the mature GaAs growth and processing technology, large area LWIR QWIP FPAs have demonstrated high uniformity and high operability, as shown in the above example. The uncorrected response nonuniformity for the 256×256 pixel array is 1 to 3 percent with an operability greater than 99.5 percent [39]. For the 128×128 pixel 15-μm array by the Jet Propulsion Laboratory [10], the uncorrected standard deviation is 2.4 percent and the corrected nonuniformity, 0.05 percent.

Nonuniformity and operability have been an issue for MCT. One of the major problems is the nonuniformity of the dark current and spectral response related to the material properties and device quality, especially at LWIR and VLWIR. MBE technology has helped in improving the uniformity in MCT arrays. For example, a 128×128 pixel LWIR array by Rockwell [4] has achieved 97.7 percent operability and 0.017 percent corrected nonuniformity. At VLWIR, the uncorrected nonuniformity of the 128×128 pixel array by Rockwell [6] is 10 percent, with 98.85 percent operability. By looking at the material and device properties, one can see that it is very hard for MCT to compete with QWIP for high uniformity and operability in a large area array format, especially at low temperature and VLWIR.

6.2 NEDT and NEI

NEDT is the minimum temperature change of a scene required to produce a signal equal to the rms noise. The importance of the uniformity for thermal imaging can be reflected by NEDT, as described by Levine [7]. When the D^* is approaching a certain limit, increasing D^* will no longer increase NEDT. The nonuniformity factor becomes the major parameter, and an improvement of nonuniformity from 0.1 percent to 0.01 percent after correction could lower the NEDT from 63 to 6.3 mK.

For low background applications, NEI is commonly used as a figure of merit. It is the radiant flux density necessary to produce a signal equal to the rms noise. The relationship between the NEI and NEDT is very simple: NEDT = NEI $\times$ $(dP_b/dT)^{-1}$, where P_b is the background photon flux. Levine's argument [7] about how nonuniformity affects NEDT is still valid for NEI. When the array is nonuniformity limited, NEI is proportional to the nonuniformity factor U. When U is reduced, a lower NEI is obtained. The BLIP operation is very difficult to achieve at very low background. In this situation, NEI is limited by the temporal noise in which the dark current nonuniformity plays an important role in device performance [40].

6.3 Bias Voltage and Impedance Match

Another factor that adds to MCT's nonuniformity is the small bias voltage. The direct injection (DI) input is one of the simplest and most popular readout circuits for IR FPAs [34], but the fluctuation on the threshold voltage is around 2 percent [41]. Because the dark current and responsivity of MCT diodes are very sensitive to the bias voltage at small bias, this bias fluctuation adds extra nonuniformity to MCT array performance. A large bias is desirable in the MCT FPA operation, but it strongly depends on the material quality of the array. For a very high-quality LWIR MCT array, –1 V bias is possible with MBE growth.

The material quality of MCT is mostly reflected by the R_oA product. A small R_oA not only allows a very small bias on the array, but also gives a very small detector impedance. In order to guarantee an efficient injection and sufficient signal-to-noise ratio, the input impedance of the detector must be much larger than that of the injection circuit. Low impedance of the detector gives a smaller injection efficiency that causes extra noise—transfer inefficient noise [38]. MCT in MWIR has a R_oA product in the range of 100 kΩ/cm^2 to 10 MΩ/cm^2; this product makes it easy to match the readout circuit and it has a high injection efficiency. In the LWIR, MCT has a much smaller R_oA product compared with those of MWIR MCT and LWIR QWIP. This product makes matching the readout difficult and it has a relatively low injection efficiency. Buffered DI or a capacitor feedback transimpedance amplifier (CTIA) can be used to increase the injection efficiency. However, it also accentuates the $1/f$ noise and the operability [6], besides occupying more room and requiring higher power levels to operate.

The bias voltage on a QWIP array usually is around 2 to 3 V. A small bias fluctuation does not affect the array performance, which gives very good bias uniformity. Even though the bias on a QWIP array is much larger than that of an MCT array, the power consumption of the QWIP FPA is still negligible compared with the readout electronics. For example, a 640×480 pixel QWIP array has a tested total power consumption of <150 mW [42]. The readout power consumption is similar for QWIP and MCT, while MCT's readout consumes more power if buffered DI or CTIA is used. The impedance of QWIP is very high, at the giga ohm range at 77 K for a pixel size of 24×24 μm^2. This high impedance makes the readout design very easy in achieving low noise and high efficiency. For example, the injection efficiency of a 640×480 pixel LWIR QWIP array is 99.5 percent [9]. This high injection efficiency makes up for some of the low quantum efficiency of QWIPs, especially at low temperature operation where most injected electrons are photoelectrons.

6.4 Charge-Handling Capacity and Integration Time

The dwell time of a 2-D staring array compared with that of a scanned single-element detector is increased by the large number of elements in the array. For example, a 256×256 pixel array has over 65,000 times more signal available to it than a single-element scanned one [43]. In most detector systems, signal strength is no longer the main concern for high background applications. The charge-handling capacity of the readout and the integration time have become the major issues. The well-charge capacity is the maximum amount of charge that can be stored on the storage capacitor of each unit cell. The size of the unit cell is limited to the dimensions of the detector element in the array. For a 30×30 μm^2 pixel size, the storage capacities are limited to 1 to 5×10^7 electrons. Assuming a 5×10^7 electron storage capacity, for example, the total current density of a detector with a 30×30 μm^2 pixel size has to be smaller than 27 μA cm^{-2}, with a 33-ms integration time. If the total current density is in the 1-mA cm^{-2} range, the integration time has to be reduced to 1 ms. The integration times for the LWIR MCT are usually <100 μs. Because the noise power bandwidth $B = 1/2\ \tau_{in}$, a small integration time causes extra noise in integration. Even though QWIP has a smaller quantum efficiency, filling the charge capacitor is usually not a problem for high background applications. The optical gain could be adjusted to allow different integration times according to the requirement. For LWIR thermal imaging at $T <$ 77 K, QWIP allows a longer integration time, which gives a relatively lower NEDT. At a temperature larger than 80 K, the dark current of QWIPs is high and fills the charge capacitor very quickly. Pushing QWIP to $T > 80$ K by only optimizing the device structure is quite difficult. Both QWIP and MCT used a number of schemes to increase the effective charge capacity of the readout. QWIP arrays with 80-K operation have been demonstrated by Lockheed Martin [42] with dark current subtraction and a noise filter on the readout. However, the readout circuit is complicated and requires extra space, which limits the size of the array. Both MCT and QWIP need multiplexers for multicolor and low background readout.

6.5 Thermal Image

Achieving FPA images has been the major goal for tactical applications. Both MCT and QWIP have demonstrated thermal images at LWIR, in which QWIP arrays have better performance at lower temperature and MCT arrays can operate at $T > 77$ K. The Jet Propulsion Laboratory (JPL) also demonstrated a camera at 15 μm. A thermal image sometimes is not necessary, such as in some strategic applications where the target is unresolved throughout most of the flight. However, an image can still be used in this situation at the development stage to examine certain features of an FPA, such as the uniformity, number of dead pixels, operability, yield, integration time, $1/f$ noise, operating temperature, and cooling cycling. Although an FPA with corrected nonuniformity can produce thermal images, uncorrected FPA images sometimes give more information about the array quality and performance. Dead pixels on an array sometimes can be seen with the human eye on an uncorrected image on a screen. In the development stage, an uncorrected image is an effective and convincing way to demonstrate an FPA's quality and performance.

7. Low Background Applications

For low background applications, the major difficulty is the achievement of BLIP operation with cooled optics. An increased quantum efficiency and reduced dark current are desired at the same time. MCT has a high quantum efficiency; a reduced dark current is the major effort. QWIP needs to improve both for low background applications. Several grating schemes under study, in combination with S-QWIP structures, have the potential to increase the conversion efficiency and reduce the dark current at the same time [27]. However, the amount of dark current reduced by removing certain active materials through the grating structures is too small for low background operation. The only way to reduce dark current on a large scale is to decrease the operating temperature. QWIP's dark current reduces three orders of magnitude uniformly from 77 K to 40 K. At low temperature in MCT, the SRH mechanism dominates the dark current through defect and impurity related tunneling, and dark current becomes very nonuniform [3]. A reduction in the dark current in MCT for low background operation is difficult simply by reducing the operating temperature. The lateral collection scheme used by Rockwell improves the R_0A at 40 K to some extent [31], but the distribution of the R_0A is still spreading out to three orders of magnitude. The purification of the substrate, source material, growth, and processing conditions can improve the MCT device quality at low temperature, but this is very costly and hard to achieve. Compared with MCT, QWIP has the potential to perform better at low temperature (40 K) for low background operation.

8. VLWIR

VLWIR sensors are very important in strategic missile defenses and space applications. FPAs of 12 to 18 μm are very useful for the detection of cold objects such as ballistic missiles in midcourse [44]. When it comes to VLWIR, the band gap of the detector is even narrower and the operating temperature has to be lower to suppress the thermally excited dark current. Both of these requirements aggravate the problems associated with the MCT material. The narrower band gap makes the MCT material system more unstable and harder to control. Direct and defect-assisted tunneling current will be increased with a decreased band gap and lower operating temperature. The variation of x across the MCT wafer can be a more severe problem and cause a much larger spectral nonuniformity. For example, at 77 K, a variation of $\Delta x = 0.2$ percent gives a cutoff wavelength variation of $\Delta\lambda_c = 0.063$ μm at MWIR ($\lambda_c = 5$ μm), while the same Δx can cause cutoff wavelength variations of $\Delta\lambda_c = 0.25$ μm for LWIR (10 μm), and $\Delta\lambda_c = 0.5$ μm for VLWIR (14 μm). Therefore, the required composition control is much more stringent for LWIR and VLWIR than for MWIR. This spectral response nonuniformity due to the compositional inhomogeneity cannot be fully corrected by the two- or three-point corrections.

The extension of QWIP to VLWIR is relatively easier because there is very little change in material properties, growth, and processing. The requirement for maintaining the device performance is to lower the operating temperature. At VLWIR, the intersubband spacing of a QWIP is relatively smaller than at LWIR. Due to the lower quantum well barriers, the dark current of thermionic emission dominates at a lower temperature. In order to achieve equivalent performance of a 10-μm cutoff QWIP at 77 K, the temperature needs to be cooled down to 55 K for a 15-μm cutoff [10] and 40 K for an 18-μm cutoff [45]. An unoptimized 128×128 pixel QWIP FPA at a 15-μm cutoff wavelength has been demonstrated by JPL [10] with an NEDT of 30 mK at 45 K with 300-K background. This initial array gives excellent images with 99.9 percent operability and corrected nonuniformity of 0.05 percent. The high quality of the array demonstrated the maturity of the GaAs technology and its potential for VLWIR applications. A 128×128 pixel MCT array [6] also demonstrated operability of 98.85 percent at 8.1×10^{15} cm^{-2}-s background flux, with an uncorrected responsivity nonuniformity of 9.8 percent. Lower background will bring more nonuniformity out due to the dark current nonuniformity that has been covered to a certain extent with a relatively higher background.

It is a big challenge for both QWIPs and MCT to meet requirements of VLWIR and low background at the same time. The major challenge for QWIP is to increase the conversion efficiency, while for MCT it is to improve the nonuniformity of both dark current and responsivity. From the performance of the two arrays demonstrated, QWIP has more potential to be realized at VLWIR and low background operation.

9. Multicolor Detectors

As IR technology continues to advance, there is a growing demand for multicolor IR detectors for advanced IR systems. For military applications, multicolor detectors are needed for better target-temperature estimation and target discrimination and identification. So far, the multiple waveband measurements have been achieved with separate FPAs that have either a dichroic filter, a mechanical filter wheel, or a dithering system with a striped filter. Each of these approaches is expensive in terms of size, complexity, and cooling requirements. A single FPA with multicolor capability is desirable to eliminate the spatial alignment and temporal registration problems that exist whenever separate arrays are used. A single FPA also has the advantages of simpler optical design and reduced size, weight, and power consumption.

Both QWIP and MCT detectors offer multicolor capability in the MWIR and LWIR atmospheric window bands, while QWIP can also easily go into the VLWIR region. For MCT, a two-color, dual-band (MWIR/LWIR) detector has been demonstrated with an n-p-p-n four-layer back-to-back diode structure grown by MBE at Hughes Research Laboratory [46]. Similar efforts are also being pursued at Lockheed Martin, Texas Instrument, and Rockwell International. But in general, the device performance of the LWIR in a two-color MCT is not quite as good as in a single-color LWIR MCT device (see data in sect. 5.2). This is due to the more complicated device structures, much thicker material growth, precise layer thickness control requirement, and bias in both directions, besides the aggravated problems related to the nature of the LWIR MCT materials. Combining VLWIR into multicolor MCT is very difficult. The 128×128 pixel MCT array at 15 μm[6] uses a planar structure that is very difficult to incorporate into multicolor structures.

By employing different designs, multicolor can be achieved in QWIP without extra difficulty. Two-stack, two-color QWIPs of MWIR/LWIR have been demonstrated at the single device level with either three-terminal simultaneous registration [20], or tuning the voltage bias between MWIR and LWIR [23]. Devices with two colors show the same high performance as single-color ones. With the same principle, multistacked QWIP structures for any combination of MWIR, LWIR, or VLWIR can be achieved with a much thinner detector structure than that for MCTs. The restriction is that the operating temperature has to be at that of the longer wavelength. A two-color (MW/LW) 256×256 pixel QWIP array with a sequential readout has been demonstrated by Lockheed Martin. Within one atmospheric window, asymmetrically coupled quantum-well structures are used to achieve voltage tunable three-color detection [47], and Stark shift has been used for fine peak wavelength tuning [48]. Due to the high-quality material and mature GaAs technology, the material growth and FPA processing do not change when the multicolor is added. The narrow spectra of QWIPs eliminate more crosstalk between colors. Compared with MCT, QWIP is much more feasible to achieve for multicolor detection than MCT and may be the only way to incorporate the VLWIR into multicolor FPAs.

10. Cost

So far, all large format LWIR and VLWIR FPAs have been developed in research and development laboratories without mass production experience. The cost of an FPA depends strongly on the maturity of the technology and is reflected by the yield. The production cost varies with production quantity, and the production learning curve varies with different companies. The substrate, manufacturing equipment, and the available potential vendors also affect the price. Another major cost issue is in the process of developing IR detector arrays that are reliable with high performance capability and fast cycle times and that also are low maintenance, can be promptly delivered, and are affordable.

MCT detectors have been the center of a major industry with a worldwide turnover of billions of dollars [49]. Major efforts have been directed toward solving the material-related problems. The potential improvements in MCT FPAs rely heavily on the advancement of the MCT material growth and processing technologies. The technology is relatively mature for MWIR, but it does not fold over to LWIR or VLWIR. Development of LWIR, VLWIR, and multicolor MCT for low background, low temperature performance requires the development of ultra-high purity material growth and device processing and the extreme minimization of crystalline defects. These requirements involve a large investment of time and money. Development of VLWIR and more than two colors in MCT are extremely difficult, especially for low background applications. The ultimate challenge in producing large MCT arrays at LWIR, VLWIR, and multicolor is the reproducibility and yield. MBE growth of MCT might be able to meet the challenge, but the finished products will have very limited vendors for production, and the manufacturing costs should be higher than for QWIP.

QWIP is based on a thriving, commercial III-V material technology that is the basis of a multibillion dollar electronics industry. Because of the maturity of the GaAs growth technology and stability of the material system, no investment is needed for developing QWIP substrates, MBE growth, and processing technology. The major challenge is with the device and grating designs to improve the device performance and meet specific applications. Because there are few material problems involved, the investment needed is relatively small and the cycling time is fast. The rapid development of QWIP over the past 10 years has shown that QWIP has had lower technology development costs and should have lower production costs compared with MCT.

11. Summary

A discussion of MCT and QWIP has been given, with emphasis on the material properties, device structures, and their impact on FPA performance and applications. From the discussion, one can see that even though QWIP is a photoconductor, it has some good properties of a photodiode, such as high impedance, fast response time, long integration time, and low power consumption. It is also easy to match with the readout circuit. Because it is a photoconductor, it avoids the major problems involved in a photodiode, such as p-type doping, SRH related *g-r* tunneling, and surface and interface instabilities. The major problems in QWIP are its relatively low conversion efficiency and a relatively high thermal generation rate at $T > 77$ K. Improved device structures and readout circuits could push QWIP to $T > 80$-K operation, but it is hard to compete with MCT in this temperature range. Due to the high material quality at low temperature and in the VLWIR region, QWIP has the potential to fulfill the system requirement for low background, low temperature applications. Further study is needed to optimize the device design, improve the device performance, and extend it to VLWIR and multicolor FPAs.

MCT has a very high quantum efficiency and wide spectral bandwidth. Its thermally generated dark current is relatively low at $T > 77$ K compared with that for QWIPs. However, MCT has material-related problems that could make it sensitive to the bias, have a low operability, large nonuniformity, and low yield. MCT has the potential to be improved at LWIR for large area FPAs at high temperature operation. However, development of MCT into large area arrays at VLWIR and multicolor is very difficult and costly, especially for low temperature and low background applications.

Even though QWIP cannot compete with MCT at the single device level and at high temperature operation due to the fundamental limit associated with intersubband transition, QWIP has potential advantages over MCT for LWIR and VLWIR FPA applications in terms of the array size, uniformity, yield, cost, and reliability. QWIPs are especially promising for VLWIR at low temperature operation and when multicolor detection with a single FPA is desired. To achieve VLWIR detection at low background is a challenge for both QWIP and MCT, while for QWIP there is more potential for this to be realized.

12. Suggestion

In October 1992, a consortium was assembled and supported by the Defense Advanced Research Projects Agency (DARPA) to develop MCT with the technical approach focused on optimizing flexible MBE manufacturing and refining the procedures and processes necessary to fabricate IR FPAs with p-on-n HgCdTe double-layer heterostructures [50]. Significant progress has been achieved in MBE growth of MCT during the past five years. Even though QWIP has been developed very quickly and has the potential to be used in LWIR, VLWIR, and multicolor both for tactical and strategic applications, the resources and efforts have mostly been limited to increasing the operating temperature for tactical applications. In order to fully develop QWIP toward strategic applications, a consortium is needed, with a collaborative effort that involves Department of Defense (DoD) research labs, defense industries, and related universities. The emphasis should be on a systematic development of QWIP FPAs by refining the design and manufacturing process and carrying out a research and development effort—from device design, array fabrication, and readout integration, all the way to field testing—that leads toward specific system applications.

Acknowledgments

The content of this paper is an independent study and reflects the author's opinion. The author would like to thank W. Dyer and D. Duston for raising the issue, as well as helpful discussions, suggestions, encouragement, and corrections to the manuscript; H. Pollehn, J. Little, W. Clark, S. S. Li, and S. Kennerly for helpful discussions, suggestions, and corrections to the manuscript; X. D. Jiang for help with preparing the figures and the manuscript; Bill Woodbridge and Lisa Lacey for their time and effort in editing and preparing a camera-ready copy of this report; and L. Kozlowski, S. Bandara, S. Gunapala, R. Martin, O. Wu, W. Beck, K. Bacher, D. Hayden, S. Winterberg, A. Goldberg, D. Beekman, K. Brown, M. Dodd, N. Dahr, and C. Cockrum for helpful discussions, suggestions, and information.

References

1. L. J. Kozlowski and W. E. Kleinhans, *Proceedings of the Third International Symposium on Long Wavelength Infrared Detectors and Arrays: Physics and Applications III*, PV 95–28 (1995), p 158.
2. P. T. Compain and R. Boch, *SPIE*, **2744** (1997), p 374.
3. T. Tung, L. V. DeArmond, R. F. Herald, P. E. Herning, M. H. Kalisher, D. A. Olson, R. F. Risser, A. P. Stevens, and S. J. Tighe, *SPIE*, **1735** (1992), p 109.
4. J. Bajaj, J. M. Arias, M. Zandian, J. G. Pasko, L. J. Kozlowski, R. E. DeWames, and W. E. Tennant, *J. Electron. Mat.*, **24** (1995), p 1067.
5. Owen K. Wu, *Compound Semiconductors*, July/August (1996), p 26.
6. L. J. Kozlowski, J. M. Arias, W. V. McLevige, J. Montroy, K. Vural, W. E. Tennant, and S. E. Kohn, *Proceedings of the 1997 Meeting of the IRIS Specialty Group on Infrared Detectors* (1997).
7. B. F. Levine, *J. Appl. Phys.*, **74** (1993), p R1.
8. L. T. Claiborne, S. L. Barnes, A. J. Brouns, F. C. Case, E. Feltes, T. A. Shater, K. L. Brown, M. Sensiper, R. J. Martin, C. Chandler, and P. Vu, *Proceedings of the 1996 Meeting of the IRIS Specialty Group on Infrared Detectors* (1996).
9. S. D. Gunapala, S. V. Bandara, J. K. Liu, W. Hong, M. Sundaram, R. Carralejo, C. A. Shott, P. D. Maker, and R. E. Muller, *SPIE Proceedings*, Orlando, FL (1997).
10. S. D. Gunapala, J. S. Park, G. Sarusi, T. L. Lin, J. K. Liu, P. D. Maker, R.E.A. Muller, C. A. Shott, and T. Hoelter, *IEEE Trans. Electron. Devices*, **44** (1997), p 45.
11. A. Rogalski, *Infrared Photon Detectors*, A. Rogalski, ed. (1995), p 627.
12. W.F.H. Michlethwaite, *Semiconductor and Semimetals*, R. K. Willardson and A. C. Beer, eds. **18** (1981), p 47.
13. S. C. Shen, *Microelectronics Journal*, **25** (1994), p 713.
14. A. Rogalski, *Infrared Phys. Technol.*, **35** (1994), p 1.
15. G. Sarusi, S. D. Gunapala, J. S. Park, and B. F. Levine, *J. Appl. Phys.*, **76** (1994), p 6001.
16. B. F. Levine, A. Zussman, S. D. Gunapala, M. T. Asom, J. M. Kuo, and W. S. Hobson, *J. Appl. Phys.*, **72** (1992), p 4429.
17. Larry S. Yu and Sheng S. Li, *Appl. Phys. Lett.*, **59** (1991), p 1332.
18. Jozef Piotrowski, *Infrared Photon Detectors*, A. Rogalski, ed. (1995), p 400.
19. W. Tennant, MCT Photodiode Technology Workshop at U.S. Army Research Laboratory, Fort Monmouth, NJ (24 May 1993).

20. M. Z. Tidrow, J. C. Chiang, Sheng S. Li, and K. Bacher, *Appl. Phys. Lett.*, **70** (1997), p 859.

21. M. Z. Tidrow, *Three-Well One- and Two-Color Quantum Well Infrared Photodetectors*, Mate. Chem. and Phys., **50**, 3 (1997) p 183.

22. S. E. Schacham and E. Finkman, *SPIE*, **1106** (1989), p 198.

23. M. Z. Tidrow, K. K. Choi, A. J. DeAnni, W. H. Chang, and S. P. Svensson, *Appl. Phys. Lett.*, **67** (1995) p 1800.

24. L. Lundqvist, J. Y. Andersson, Z. F. Paska, J. Borglind, and D. Haga, *Appl. Phys. Lett.*, **63**, 3361 (1993).

25. J. E. Scheihing and M. A. Dodd, *Proceedings of the First International Symposium on Long Wavelength Infrared Detectors and Arrays: Physics and Applications*, (1993) p 78.

26. B. F. Levine, G. Sarusi, S. J. Pearton, K.M.S. Bandara, and R. E. Leibenguth, *Quantum Well Intersubband Transition Physics and Devices*, NATO ASI Series E, **270**, (1993) p 1.

27. M. A. Dodd, S. L. Barnes, A. J. Brouns, F. C. Case, L. T. Claiborne, and M. Z. Tidrow, *Proceedings of the 1997 Meeting of the IRIS Specialty Group on Infrared Detectors* (1997).

28. W. A. Beck, D. Prather, M. Mirotznick, and T. S. Faska, *Proceedings of the 5th International Symposium on LWIR Detectors and Arrays* (1997).

29. C. J. Chen, K. K. Choi, M. Z. Tidrow, and D. C. Tsui, *Appl. Phys. Lett.* **68** (1996), p 1446.

30. M. Z. Tidrow and K. Bacher, *Appl. Phys. Lett.*, **69** (1996), p 3396.

31. W. V. McLevige, D. D. Edwall, J. G. Pasko, J. Bajaj, L. O. Bubulac, J. T. Viola, W. E. Tennant, K. Vural, J. Ellsworth, H. Vydyanath, R. K. Purvis, S. E. Anderson, and R. A. Ramos, *Proceedings of the 1995 Meeting of the IRIS Specialty Group on Infrared Detectors* (1995).

32. G. Destefanis and J. P. Chamonal, *J. Electron. Mater.*, **22** (1993), p 1027.

33. O. K. Wu, *Proceedings of the Third International Symposium on Long Wavelength Infrared Detectors and Arrays: Physics and Applications III* (1995), p 33.

34. A. Hairston, F. Edwards, P. Kimball-Taylor, F. Jaworski, M. B. Reine, R. Starr, M. H. Weller, M. Kestigian, B. L. Musicant, P. Mitra, *Proceedings of the IRIS Detector Specialty Group Meeting*, Boulder, CO (15–16 August 1994).

35. M. A. Kinch and A. Yariv, *Appl. Phys. Lett.*, **55** (1989), p 2093.

36. K. K. Choi, C. Y. Lee, M. Z. Tidrow, W. H. Chang, and S. D. Gunapala, *Appl. Phys. Lett.*, **65** (1994), p 1703.

37. A. Rogalski, *SPIE*, **2225** (1994), p 118.

38. M. Kimata and N. Tubouchi, *Infrared Photon Detectors*, A. Rogalski, ed. (1995), p 99.

39. W. A. Beck, T. S. Faska, J. W. Little, A. C. Goldberg, J. Albritton, and M. Sensiper, *Proceedings of the Third International Symposium on Long Wavelength Infrared Detectors and Arrays: Physics and Applications III* (1995), p 7.

40. R. L. Whitney, K. F. Cuff, and F. W. Adams, *Semiconductor Quantum Wells and Superlattices for Long-Wavelength Infrared Detectors*, M. O. Manasreh, ed., Artech House, Norwood, MA (1993), p 55.

41. P. E. Allen and D. R. Holberg, *CMOS Analog Circuit Design,* Holt, Rinehart and Winston (1987), p 99.

42. W. A. Beck and T. S. Faska, *SPIE*, **2744** (1996), p 193.

43. J. T. Wimmers and D. S. Smith, *Photonics Spectra* (December 1994).

44. D. Duston, *BMD Monitor* (19 May 1995), p 180.

45. C. Y. Lee, M. Z. Tidrow, K. K. Choi, W. H. Chang, F. J. Towner, and J. S. Ahearn, *J. Appl. Phys.*, **75** (1994), p 4731.

46. O. K. Wu, R. D. Rajavel, T. J. DeLyon, J. E. Jensen, C. A. Cockrum, S. M. Johnson, G. M. Venzor, G. R. Chapman, J. A. Wilson, E. A. Patten, and W. A. Radford, *SPIE*, **2685** (1996), p 16.

47. M. Z. Tidrow, K. K. Choi, C. Y. Lee, W. H. Chang, F. J. Towner, and J. S. Ahearn, *Appl. Phys. Lett.*, **64** (1994), p 1268.

48. Jung-Chi Chiang, Sheng S. Li, M. Z. Tidrow, P. Ho, C. M. Tsai, and C. P. Lee, *Appl. Phys. Lett.*, **69** (1996), p 2412.

49. E. D. Carlton, *J. Cryst. Growth*, **59** (1982), p 98.

50. J. D. Benson, et al, *SPIE*, **2744** (1996), p 126.

Distribution

Admnstr
Defns Techl Info Ctr
Attn DTIC-OCP
8725 John J Kingman Rd Ste 0944
FT Belvoir VA 22060-6218

Ballistic Mis Defns Org
Attn D Duston
Attn W Dyer
7100 Defense The Pentagon
Washington DC 20301-7100

Inst for Defns Analyses Sci & Techlgy Div
Attn G Hopper
Attn K Carson
Attn R Singer
1801 N Beauregard Stret
Alexandria VA 22311-1772

Ofc of the Dir Rsrch and Engrg
Attn R Menz
Pentagon Rm 3E1089
Washington DC 20301-3080

Ofc of the Secy of Defns
Attn ODDRE (R&AT) G Singley
Attn ODDRE (R&AT) S Gontarek
The Pentagon
Washington DC 20301-3080

OSD
Attn OUSD(A&T)/ODDDR&E(R) R Tru
Washington DC 20301-7100

AMCOM MRDEC
Attn AMSMI-RD W C McCorkle
Redstone Arsenal AL 35898-5240

Army Rsrch Ofc
Attn AMXRO-GS Bach
Attn H Everitt
PO Box 12211
Research Triangle Park NC 27709

Army Rsrch Ofc
Attn M Stroscio
4300 S Miami Blvd
Research Triangle Park NJ 27709

Army Rsrch Physics Div
Attn AMXRO-PH D Skatrud
Research Triangle Park NC 27709

CECOM
Attn PM GPS COL S Young
FT Monmouth NJ 07703

CECOM
Sp & Terrestrial Commctn Div
Attn AMSEL-RD-ST-MC-M H Soicher
FT Monmouth NJ 07703-5203

DARPA
Attn R Balcerak
3701 N Fairfax Dr
Arlington VA 22203-1714

Dir for MANPRINT
Ofc of the Deputy Chief of Staff for Prsnnl
Attn J Hiller
The Pentagon Rm 2C733
Washington DC 20301-0300

Dpty Assist Secy for Rsrch & Techl
Attn SARD-TT F Milton Rm 3E479
The Pentagon
Washington DC 20301-0103

Hdqtrs Dept of the Army
Attn DAMO-FDT D Schmidt
400 Army Pentagon Rm 3C514
Washington DC 20301-0460

Night Vision & Elec Sensors Dir
Attn AMSEL-RD-NV-OD J Ratches
Attn AMSEL-RD-NV-OV J Pollard
10221 Burbeck Rd Ste 430
FT Belvoir VA 22060-5806

TECOM
Attn AMSTE-CL
Aberdeen Proving Ground MD 21005-5057

US Army CECOM
Rsrch, Dev, & Engrg Ctr
Attn R Buser
FT Monmouth NJ 07703-5201

Distribution (cont'd)

US Army Edgewood
Rsrch, Dev, & Engrg Ctr
Attn SCBRD-TD J Vervier
Aberdeen Proving Ground MD 21010-5423

US Army Info Sys Engrg Cmnd
Attn ASQB-OTD F Jenia
FT Huachuca AZ 85613-5300

US Army Materiel Sys Analysis Agency
Attn AMXSY-D J McCarthy
Aberdeen Proving Ground MD 21005-5071

US Army Matl Cmnd
Dpty CG for RDE Hdqtrs
Attn AMCRD BG Beauchamp
5001 Eisenhower Ave
Alexandria VA 22333-0001

US Army Matl Cmnd
Prin Dpty for Acquisition Hdqrts
Attn AMCDCG-A D Adams
5001 Eisenhower Ave
Alexandria VA 22333-0001

US Army Matl Cmnd
Prin Dpty for Techlgy Hdqrts
Attn AMCDCG-T M Fisette
5001 Eisenhower Ave
Alexandria VA 22333-0001

US Army Natick Rsrch, Dev, & Engrg Ctr
Acting Techl Dir
Attn SSCNC-T P Brandler
Natick MA 01760-5002

US Army Simulation, Train, & Instrmntn Cmnd
Attn J Stahl
12350 Research Parkway
Orlando FL 32826-3726

US Army Tank-Automtv & Armaments Cmnd
Attn AMSTA-AR-TD C Spinelli
Bldg 1
Picatinny Arsenal NJ 07806-5000

US Army Tank-Automtv Cmnd
Rsrch, Dev, & Engrg Ctr
Attn AMSTA-TA J Chapin
Warren MI 48397-5000

US Army Test & Eval Cmnd
Attn R G Pollard III
Aberdeen Proving Ground MD 21005-5055

US Army Train & Doctrine Cmnd
Battle Lab Integration & Techl Dirctrt
Attn ATCD-B J A Klevecz
FT Monroe VA 23651-5850

US Military Academy
Dept of Mathematical Sci
Attn MAJ D Engen
West Point NY 10996

Nav Rsrch Lab
Attn Code 6818 J Omaggio
Washington DC 20375

Nav Rsrch Lab
Attn Code 5636 M Kruer
4555 Overlook Ave
Washington DC 20375-5000

Nav Surface Warfare Ctr
Attn Code B07 J Pennella
17320 Dahlgren Rd Bldg 1470 Rm 1101
Dahlgren VA 22448-5100

NVESD
Attn AMSEL-RD-NV-ST-IRT S Horn
10221 Burbeck Rd
FT Belvoir VA 22060-5806

AFOSR/NE
Attn M Prarie
110 Duncan Ave Ste B115
Bolling AFB DC 20332-6448

GPS Joint Prog Ofc Dir
Attn COL J Clay
2435 Vela Way Ste 1613
Los Angeles AFB CA 90245-5500

US Air Force Phillips Lab
Attn PL/VTE R Pugh
Attn PL/VTE P LeVan
3550 Aberdeen Ave SE
Kirtland AFB NM 87117

Distribution (cont'd)

DARPA
Attn B Kaspar
Attn L Stotts
3701 N Fairfax Dr
Arlington VA 22203-1714

NASA Goddard Solid State Device Dev Br
Attn Code 718 M Jhabvala
Bldg 11 Rm E23
Greenbelt MD 20771

Lockheed Martin Sanders
Attn MS NHQ 6-1517 J Ahearn
65 Spit Brooke Rd
Nashua NH 03061-0868

Palisades Inst for Rsrch Svc Inc
Attn E Carr
1745 Jefferson Davis Hwy Ste 500
Arlington VA 22202-3402

Rockwell Internatl Sci Ctr Elect Dev Lab
Attn B Tennant
1049 Camimo Dos Rios
Thousand Oaks CA 91360

SRI Internatl
Attn A Sher
333 Ravenswood Ave
Menlo Park CA 94025

US Army Rsrch Lab
Attn J Zavada
PO Box 12211
Research Triangle Park NC 27709-2211

US Army Rsrch Lab
Attn AMSRL-CI-LL Techl Lib (3 copies)
Attn AMSRL-CS-AL-TA Mail & Records Mgmt
Attn AMSRL-CS-AL-TP Techl Pub (3 copies)
Attn AMSRL-SE-EE B Beck
Attn AMSRL-SE-EI M Tidrow (20 copies)
Adelphi MD 20783-1197

REPORT DOCUMENTATION PAGE

Form Approved
OMB No. 0704-0188

1. AGENCY USE ONLY *(Leave blank)*	2. REPORT DATE	3. REPORT TYPE AND DATES COVERED
	May 1998	Summary, November 1996–July 1997

4. TITLE AND SUBTITLE

QWIP and MCT for Long Wavelength and Multicolor Focal Plane Array Applications

5. FUNDING NUMBERS

PE: 62120A

6. AUTHOR(S)

Meimei Z. Tidrow

7. PERFORMING ORGANIZATION NAME(S) AND ADDRESS(ES)

U.S. Army Research Laboratory
Attn: AMSRL-SE-EI (mtidrow@arl.mil)
Adelphi, MD 20783-1197

8. PERFORMING ORGANIZATION REPORT NUMBER

ARL-TR-1534

9. SPONSORING/MONITORING AGENCY NAME(S) AND ADDRESS(ES)

Ballistic Missile Defense Organization
7100 Defense Pentagon, Room 1E149
Washington, DC 20301-7100

10. SPONSORING/MONITORING AGENCY REPORT NUMBER

11. SUPPLEMENTARY NOTES

AMS code: 622120.H16
ARL PR: 7NBBBB

12a. DISTRIBUTION/AVAILABILITY STATEMENT

Approved for public release; distribution unlimited.

12b. DISTRIBUTION CODE

13. ABSTRACT *(Maximum 200 words)*

Infrared (IR) sensor technology is critical to all phases of ballistic missile defense. Traditionally, material systems such as indium antimonide (InSb), platinum silicide (PtSi), mercury cadmium telluride (MCT), and arsenic doped silicon (Si: As) have dominated IR detection. Improvement in surveillance sensors and interceptor seekers requires large, highly uniform, and multicolor (or multi-spectral) IR focal plane arrays involving mid-wave (MW), long-wave (LW), and very-long-wave (VLW) IR regions. Among the competing technologies are quantum-well infrared photodetectors (QWIPs) based on lattice-matched GaAs/AlGaAs and strained layer InGaAs/AlGaAs material systems. Even though QWIP cannot compete with MCT at the single device level (considering the quantum efficiency and D^*), it has potential advantages over MCT for LW and VLW focal plane array applications in terms of the array size, uniformity, operability, yield, reliability, and cost effectiveness. QWIPs are especially promising for VLWIR at low temperature operation, and when simultaneous multicolor detection with a single focal plane array is desired. Operating a VLWIR focal plane array at low background is a challenge to both MCT and QWIP, while QWIP has more potential to be realized due to its good properties at low temperatures. In this paper, I discuss cooled IR technology with an emphasis on QWIP and MCT. I give details concerning device physics, material growth, device fabrication, device performance, and cost effectiveness for LWIR, VLWIR, and multicolor applications.

14. SUBJECT TERMS

QWIP, MCT, FPA, IR detectors

15. NUMBER OF PAGES

37

16. PRICE CODE

17. SECURITY CLASSIFICATION OF REPORT	18. SECURITY CLASSIFICATION OF THIS PAGE	19. SECURITY CLASSIFICATION OF ABSTRACT	20. LIMITATION OF ABSTRACT
Unclassified	Unclassified	Unclassified	SAR